# ORIGINAL ARTICLE



# Phytophthora infestans RXLR effector Pi23014 targets host RNA-binding protein NbRBP3a to suppress plant immunity

Wanyue Li<sup>1</sup> | Zeming Liu<sup>1</sup> | Yuli Huang<sup>1</sup> | Jie Zheng<sup>1</sup> | Yang Yang<sup>1,2</sup> | Yimeng Cao<sup>1</sup> | Liwen Ding<sup>1</sup> | Yuling Meng<sup>1</sup> | Weixing Shan<sup>1,2</sup>

<sup>1</sup>State Key Laboratory for Crop Stress Resistance and High-Efficiency Production, and College of Agronomy, Northwest A&F University, Yangling, Shaanxi, China

<sup>2</sup>State Key Laboratory for Crop Stress Resistance and High-Efficiency Production, and College of Plant Protection, Northwest A&F University, Yangling, Shaanxi, China

#### Correspondence

Weixing Shan, State Key Laboratory for Crop Stress Resistance and High-Efficiency Production, College of Agronomy and College of Plant Protection, Northwest A&F University, Yangling, Shaanxi 712100, China. Email: wxshan@nwafu.edu.cn

#### **Funding information**

China Agriculture Research System, Grant/Award Number: CARS-09; Program of Introducing Talents of Innovative Discipline to Universities from the State of Administration for Foreign Experts Affairs, China, Grant/Award Number: #B18042; Agricultural Breeding program, Grant/ Award Number: 2019NYYZ01

#### **Abstract**

Phytophthora infestans is a destructive oomycete that causes the late blight of potato and tomato worldwide. It secretes numerous small proteins called effectors in order to manipulate host cell components and suppress plant immunity. Identifying the targets of these effectors is crucial for understanding P. infestans pathogenesis and host plant immunity. In this study, we show that the virulence RXLR effector Pi23014 of P. infestans targets the host nucleus and chloroplasts. By using a liquid chromatogrpahytandem mass spectrometry assay and co-immunoprecipitation assasys, we show that it interacts with NbRBP3a, a putative glycine-rich RNA-binding protein. We confirmed the co-localization of Pi23014 and NbRBP3a within the nucleus, by using bimolecular fluorescence complementation. Reverse transcription-quantitative PCR assays showed that the expression of NbRBP3a was induced in Nicotiana benthamiana during P. infestans infection and the expression of marker genes for multiple defence pathways were significantly down-regulated in NbRBP3-silenced plants compared with GFP-silenced plants. Agrobacterium tumefaciens-mediated transient overexpression of NbRBP3a significantly enhanced plant resistance to P. infestans. Mutations in the N-terminus RNA recognition motif (RRM) of NbRBP3a abolished its interaction with Pi23014 and eliminated its capability to enhance plant resistance to leaf colonization by P. infestans. We further showed that silencing NbRBP3 reduced photosystem II activity, reduced host photosynthetic efficiency, attenuated Pi23014-mediated suppression of cell death triggered by P. infestans pathogen-associated molecular pattern elicitor INF1, and suppressed plant immunity.

#### **KEYWORDS**

glycine-rich RNA-binding protein, Phytophthora infestans, Pi23014, PSII activity, PTI, RXLR effectors

Wanyue Li and Zeming Liu contributed equally.

This is an open access article under the terms of the Creative Commons Attribution-NonCommercial License, which permits use, distribution and reproduction in any medium, provided the original work is properly cited and is not used for commercial purposes. © 2024 The Authors. Molecular Plant Pathology published by British Society for Plant Pathology and John Wiley & Sons Ltd.

### 1 | INTRODUCTION

Plants have developed complex mechanisms to compensate for and respond to changing environmental conditions (Tsuda & Lu, 2020). Pathogen infection may limit plant growth and productivity, leading to serious loss of crop yield (Kachroo et al., 2021; Ngou et al., 2021). To successfully infect a plant, pathogens often need to evade host detection and suppress immune responses. The plant immune system consists of two defence layers: pathogen-associated molecular pattern (PAMP)-triggered immunity (PTI) and effector-triggered immunity (ETI) (Jones & Dangl, 2006; Wang, Feng, et al., 2020).

Post-transcriptional regulatory mechanisms underlying the ability of plants to respond and adapt to environmental changes have received significant attention, leading to the identification of RNA-binding proteins (RBPs) as key regulators of growth, development and responses to environmental stress (Lee & Kang, 2016; Prall et al., 2019). The RBPs are directly or indirectly involved in the regulation of post-transcriptional RNA metabolism (Mahalingam & Walling, 2020). The RBPs are characterized by the presence of putative RNA-binding domains, such as RNA recognition motifs and K homology domains, DEAD/DEAH box domains, glycinerich domains, arginine-rich domains and serine-rich domains (Zuo et al., 2019).

A number of putative RBPs have been implicated as regulators of plant immunity by modulating cellular metabolism and regulating gene expression during biotic stress (Zhang et al., 2022). For example, silencing of the RBP TaCSP41a decreases wheat susceptibility to *Puccinia striiformis* f. sp. *tritici* (Corredor-Moreno et al., 2022). TaRZ1, a zinc finger-containing glycine-rich RBP, has been shown to enhance resistance to *Pseudomonas syringae* pv. *tomato* DC3000. The expression of *TaRZ1* in *Arabidopsis* also affects many genes related to plant growth and stress response (Xu et al., 2015). RBP StUBA2a/b also positively regulates plant defence against *Phytophthora* pathogens via the salicylic acid (SA) signalling pathway (Li et al., 2022).

In addition, glycine-rich RNA-binding proteins (GR-RBPs), which contain an RRM at the N-terminus and a glycine-rich region at the C-terminus, play an important role in the regulation of posttranscriptional gene expression in plants undergoing biotic stress (Lee & Kang, 2016; Mahalingam & Walling, 2020). RBPs contain an RRM and additional domains necessary for mediating protein-protein interactions, as well as regulating post-transcriptional modification (Tang et al., 2021). NbGRP7 interacts with the NB-LRR immune receptor Rx1, which confers resistance to potato virus X by regulating Rx1 transcript abundance. RRM mutations in NbGRP7 attenuate its role in Rx1-mediated defence, suggesting that the RRM motif may be the key to the function of NbGRP7 in NB-LRR-mediated immunity (Oca et al., 2022). CaGRP1 negatively regulates CaPIK1-triggered cell death and defence responses by suppressing reactive oxygen species (ROS) accumulation (Kim et al., 2015). StUBA2s induces cell death in tobacco leaves through its RRM domain and regulates immunity by affecting the expression of pathogen-related genes

(PR) and senescence-related genes (SAG13) (Jong-Kuk et al., 2015). PigmR, which mediated rice resistance to *Magnaporthe oryzae*, was found to interact with the RRM-containing protein PIBP1. PIBP1 is required for complete blast resistance by directly interacting with the conserved CC domains of NLRs that confer resistance to a broad spectrum of blast races. PIBP1 and its homologue Os06G02240 are specific proteins that mediate PigmR and other broad-spectrum NLR resistance (Zhai et al., 2019). As more studies on this interaction are conducted, RBPs are increasingly recognized as potential targets for crop breeding.

Pathogen effectors have been found to regulate plant immunity by targeting RBPs. The ADP-ribosylation of RBP GRP7 by the bacterial pathogen *P. syringae* pv. tomato DC3000 effector HopU1 requires the RRM (Fu et al., 2007). HopU1 was further shown to inhibit the function of GRP7 in PTI (Nicaise et al., 2013). The potato RBP StKRBP1 has been identified as a target of the *P. infestans* effector Pi04089, an important susceptibility factor for colonization by the late blight pathogen (Wang et al., 2015). RBPs are frequently targeted by effectors to manipulate plant immunity (Manavski et al., 2018).

Previous studies have shown that *P. infestans* employs its RXLR effector Pi23014 to suppress plant defence responses and promote disease (Huang et al., 2020; Wang et al., 2019). In this work, we report the identification of NbRBP3a, a positive immune regulator targeted by the chloroplast-localized effector protein Pi23014. We investigated the effect of NbRBP3a on photosystem II (PSII) activity and the expression of PSII-related protein genes. Deletion of the RNA recognition motif in the N-terminus of NbRBP3a abolished its interaction with Pi23014 and immune function. Our results reveale that NbRBP3a positively regulated plant defence responses to *P. infestans* by activating PTI.

# 2 | RESULTS

# 2.1 | The *P. infestans* effector Pi23014 targets NbRBP3a

Pi23014 is an RXLR effector and virulence factor of *P. infestans* (Figure S1), which is identical in protein sequence with Pi23015 (Huang et al., 2020; Wang et al., 2019). To further reveal the molecular mechanisms by which Pi23014 inhibits plant defence responses, we employed liquid chromatography-tandem mass spectrometry (LC-MS/MS) assays to quickly obtain candidate host target proteins (Table S1).

We found that the coverage of NbRBP3a was 52% and NbRBP3a showed four unique peptides on the mass spectrometer experiments (Table S1). A BLAST search showed the presence of three NbRBP3 homologue genes, Niben101Scf09268g00007.1 (NbRBP3a), Niben101Scf04659g00004.1 (NbRBP3b) and Niben101Scf05279g01002.1 (NbRBP3c) in Nicotiana benthamiana (Figure S2). The expression of NbRBP3 genes in response to P. infestans infection was examined at different time points using

reverse transcription-quantitative PCR (RT-qPCR) assays. Notably, the expression levels of NbRBP3a were significantly up-regulated by at least 200-fold at 6h post-inoculation (hpi) with P. infestans zoospores on N. benthamiana leaves in three independent biological experiments (Figure S3), while the expression levels of NbRBP3b and NbRBP3c were no more than three- and fivefold at any given time during infection, respectively (Figure S3). Bioinformatic analysis showed that NbRBP3a contains an RRM motif at the N-terminus and a glycine-rich region at the C-terminus (Figure S4).

To investigate the interaction between Pi23014 and NbRBP3a, we performed firefly luciferase complementation imaging (LCI) assays in N. benthamiana leaves. We also constructed a series of mutants, including NbRBP3a\Delta C that was modified by a deletion of the C-terminus glycine-rich region, and NbRBP3a∆N that lacked the N-terminus RRM (Figure S4). The results showed strong luminescence signals on leaves in which nlucPi23014 was co-expressed with clucNbRBP3a or clucNbRBP3aΔC, respectively (Figures 1a and S5). No luminescence signals were detected in the negative controls, nor did nlucPi23014 and clucNbRBP3a∆N, indicating that the NbRBP3a\D mutant form no longer interacted with Pi23014.

We also tested the interaction between Pi23014 and NbRBP3a through yeast two-hybrid (Y2H) assays. While all yeast transformants grew on SD/-Leu/-Trp medium, the interaction of Pi23014 and NbRBP3a was indicated by induction of  $\beta$ -galactosidase ( $\beta$ -Gal) activity and growth on quadruple dropout (QDO) medium (Figure 1b). The negative controls, yeast cells co-transformed with Pi23014 and NbRBP3aΔC, could not grow on QDO medium and did not show β-Gal activity, nor did Pi23014 and NbRBP3aΔN (Figure 1b).

The protein interaction was further confirmed by a bimolecular fluorescence complementation (BiFC) assay. Co-expression by agroinfiltration-mediated assays in N. benthamiana leaves was performed with N-terminus of yellow fluorescent protein (YFP) (nYFP) in Pi23014 and C-terminus of YFP (cYFP) in NbRBP3a, NbRBP3a∆C and NbRBP3a\Delta N, respectively. The fluorescence signals were observed specifically in the nucleus at 48h post-agroinfiltration, indicating that Pi23014 interacted with NbRBP3a and NbRBP3a∆C (Figures 1c and S6). Fluorescence was not observed in the coexpression of Pi23014 and NbRBP3a∆N (Figures 1c and S6). These results indicated that the physical interaction between Pi23014 and NbRBP3a mostly occurred in the plant nucleus.

Furthermore, we performed a co-immunoprecipitation (Co-IP) assay to confirm the interaction between Pi23014 and NbRBP3a. The mCherry tag was fused to the C-terminus of the NbRBP3a and its mutants (NbRBP3a $\Delta$ C and NbRBP3a $\Delta$ N). These fusion proteins were transiently expressed in N. benthamiana leaves with either Pi23014-CGFP or green fluorescent protein (GFP) via agroinfiltration. The Co-IP results showed that NbRBP3a-CmCherry and NbRBP3aΔC-CmCherry were immunoprecipitated with Pi23014-CGFP, but not with GFP, respectively (Figures 1d and S7). NbRBP3a∆N-CmCherry was not immunoprecipitated with Pi23014-CGFP, nor with GFP (Figures 1d and S7). Taken together, these results confirmed that the specific association between Pi23014 and NbRBP3a in plants depends on the RNA recognition motif.

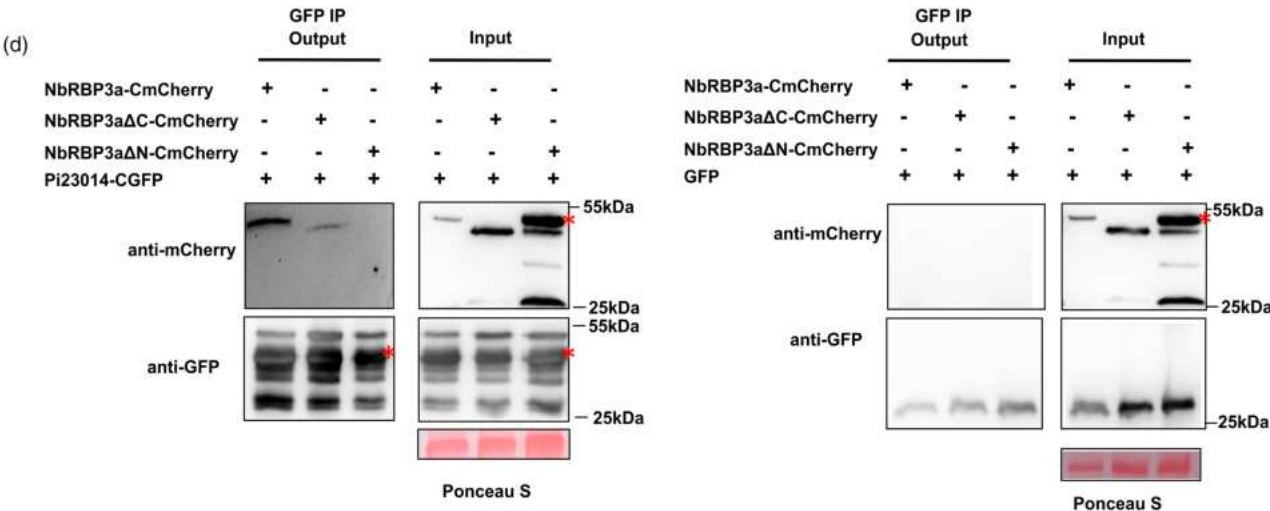
# 2.2 | Pi23014-NbRBP3a interaction occurs in the nucleus

We further analysed the localization of NbRBP3a. Transient expression assays were performed for GFP-fused NbRBP3a constructs in N. benthamiana. A clear GFP signal was detected by confocal microscopy in the nucleus and network-like structures (Figures 2a and S8). To further determine this network-like structure, we examined the localization of NbRBP3a-CGFP with the mCherry-labelled endoplasmic reticulum (ER) marker (Fan et al., 2018). We noted that NbRBP3a-CGFP overlapped with the ER marker but not completely (Figures 2a and S8), indicating that the function of NbRBP3a may be related to the ER. These results showed that NbRBP3a-CGFP, NbRBP3a\DC-CGFP and NbRBP3a\DN-CGFP, shared the same subcellular localization when observed using confocal fluorescence microscopy (Figures 2a and S8).

To determine the subcellular localization of Pi23014 in association with NbRBP3a, we performed transient co-expression assays in N. benthamiana. We found that the fusion effector protein Pi23014-CGFP accumulated mainly in the nucleus and the chloroplastassociated structures (Figure S1). Our results determined that Pi23014-CGFP and NbRBP3a-CmCherry, NbRBP3aΔC-CmCherry and NbRBP3a∆N-CmCherry all co-localized in the nucleus under the confocal fluorescence microscopy (Figure 2b). Pi23014 did not affect the localization of NbRBP3a, NbRBP3aΔC and NbRBP3aΔN. The expression and integrity of fusion proteins were confirmed by western blotting using appropriate antibodies (Figure S9).

# The RRM motif of NbRBP3a is essential for plant resistance

To further examine the immune function of NbRBP3 genes in plants, virus-induced gene silencing (VIGS) was used to generate NbRBP3 knock-down N. benthamiana plants. Due to their high similarity in gene sequences, we selected the common region of NbRBP3a, NbRBP3b and NbRBP3c for silencing to avoid functional redundancy in N. benthamiana (Figure S2). It is notable that the TRV-NbRBP3 silenced plants showed mottled yellow leaves and retarded growth (Figures S10 and S11). RT-qPCR assay was used to confirm silencing efficiency, with results showing that NbRBP3a, NbRBP3b and NbRBP3c transcript levels were reduced by 60%-80% (Figure S10). Infection assays with P. infestans zoospores showed that the TRV-NbRBP3 silenced plants developed significantly larger lesions compared to the control TRV-GFP silenced plants (Figure 3a). This result indicated that silencing NbRBP3 increased plant susceptibility. These results were consistent with P. infestans biomass quantification, which revealed much more pathogen colonization in the TRV-NbRBP3 silenced plants compared to the TRV-GFP silenced plants (Figure 3a). Transient overexpression in N. benthamiana followed by infection assays with P. infestans zoospores showed that NbRBP3a-CGFP significantly reduced P. infestans colonization compared to the GFP control plants at 5 days post-inoculation (dpi). This was visualized by smaller lesions in NbRBP3a -CGFP overexpression leaves (Figure 3b)



as shown by trypan blue staining, demonstrating that *NbRBP3a* contributed to plants' resistance to *P. infestans*.

NbRBP3a is a GR-RBP that contains an RRM motif at the N-terminus and a glycine-rich region at the C-terminus (Figure S4). To examine whether the RRM motif is required for the immune

function of NbRBP3a protein, mutant constructs NbRBP3a\Delta N-CGFP and NbRBP3a\Delta C-CGFP were created and transiently expressed in N. benthamiana by agroinfiltration followed by infection with P. infestans zoospores. These results showed that NbRBP3a\Delta C-CGFP had significantly reduced lesion sizes compared to the GFP plants. Alternatively,

13643703, 2024, 1, Downloaded from https://bsppjoumals

onlinelibrary.wiley.com/doi/10.1111/mpp.13416 by Readcube-Labtiva, Wiley Online Library on [20/09/2025]. See the Terms

of use; OA articles are governed by the applicable Creative Commons Licen

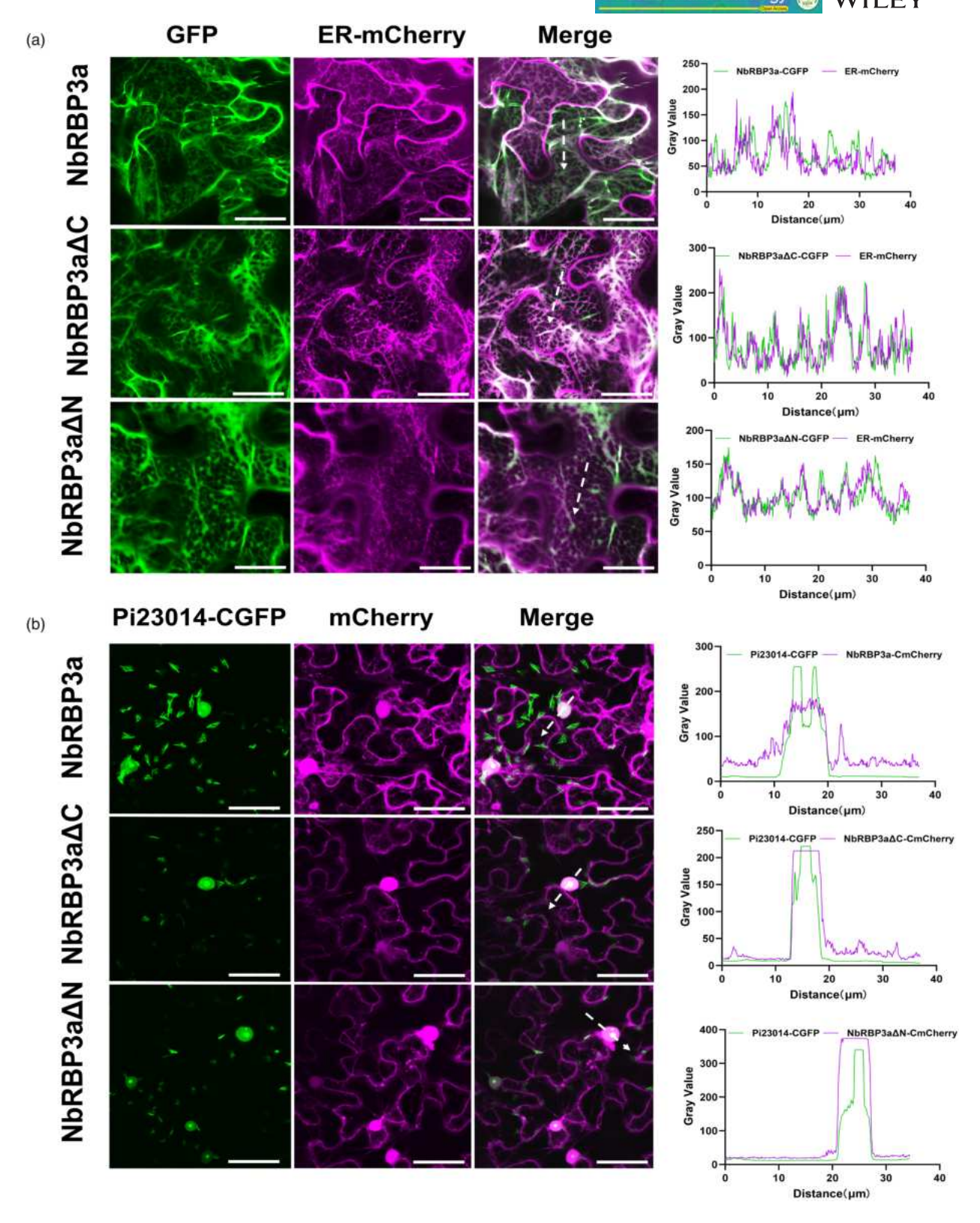


FIGURE 2 Co-localization of Pi23014 and NbRBP3a in the host plant nucleus. NbRBP3a-CGFP, NbRBP3a $\Delta$ C-CGFP, and NbRBP3a $\Delta$ N-CGFP were transiently co-expressed with ER-mCherry marker in Nicotiana benthamiana by agroinfiltration (a). NbRBP3a-CmCherry, NbRBP3a $\Delta$ C-CmCherry, and NbRBP3a $\Delta$ N-CmCherry were transiently co-expressed with Pi23014-CGFP, respectively, in N. benthamiana by agroinfiltration (b). Photographs were taken 2 days after agroinfiltration. Bars, 40  $\mu$ m. The white arrows show the lines used for the fluorescence intensity profiles of single optical section indicated in the images.

3643703, 2024, 1, Downloaded from https://bsppjournals

onlinelibrary.wiley.com/doi/10.1111/mpp.13416 by Readcube-Labtiva, Wiley Online Library on [20/09/2025]. See the Terms and Conditions

ons) on Wiley Online Library for rules of use; OA articles are governed by the applicable Creative Commons Licens

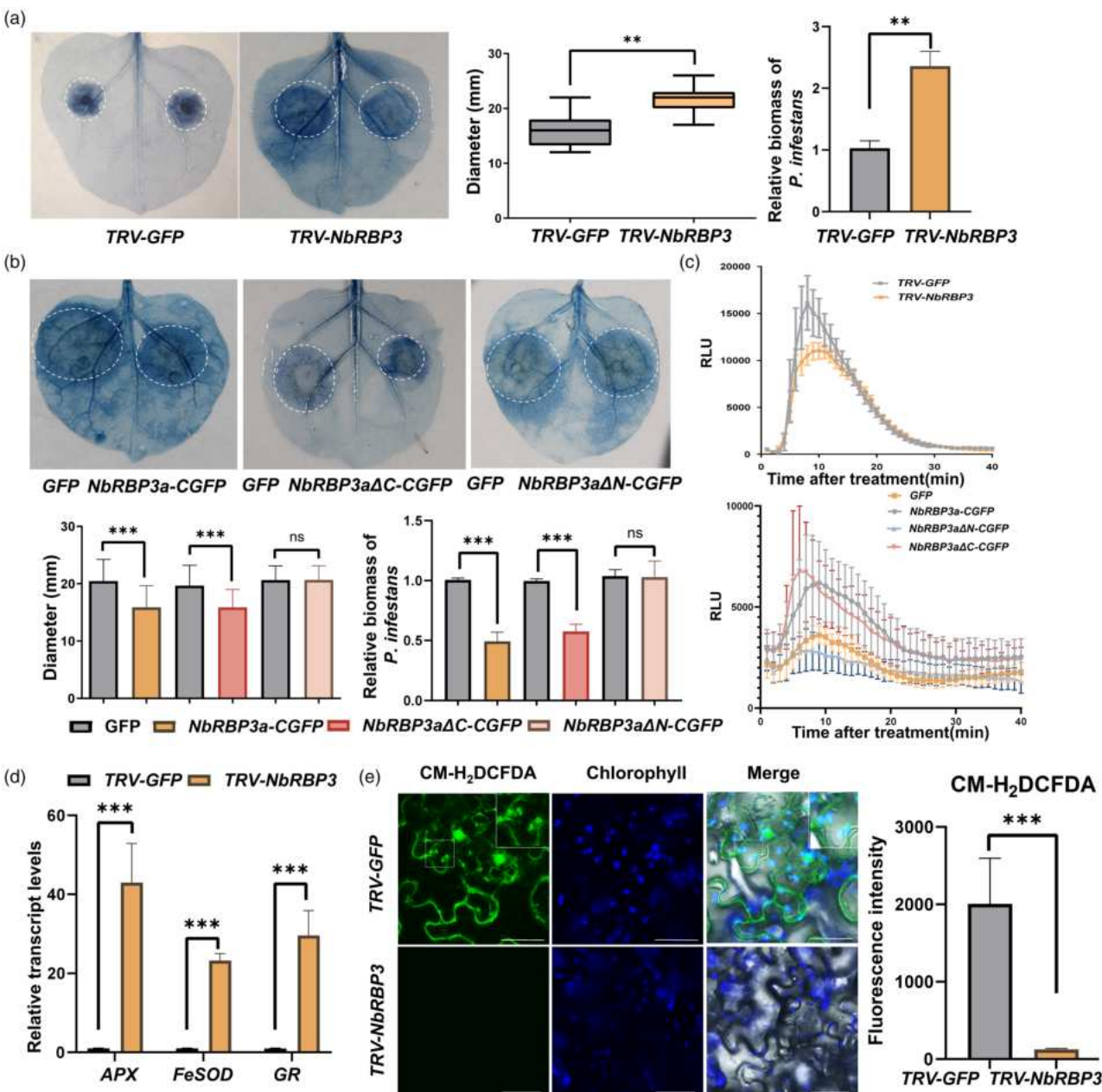


FIGURE 3 NbRBP3a positively regulated plant resistance to Phytophthora infestans. (a)TRV-NbRBP3 silenced plants inoculated with P. infestans zoospores were scored. The lesion size and P. infestans biomass were quantified at 5 days post-inoculation (dpi). The infected leaves were stained with trypan blue to highlight the lesions. At least 10 leaves were used for statistical analysis. (b) P. infestans infection assays on Nicotiana benthamiana leaves overexpressing NbRBP3a-CGFP, NbRBP3a $\Delta$ C-CGFP, NbRBP3a $\Delta$ N-CGFP, respectively, were scored. The lesion size and P. infestans biomass were quantified at 5 dpi. Lesion diameter and P. infestans biomass were based on Student's t-test. At least 10 leaves were used for statistical analysis. Asterisks above the bars indicate significant differences (\*\*p < 0.01, \*\*\*p < 0.001; ns, no significance). (c) Quantification of reactive oxygen species (ROS) production in the leaf discs of TRV-NbRBP3 silenced plants, NbRBP3α-CGFP, NbRBP3αΔC-CGFP, and NbRBP3 $a\Delta$ N-CGFP overexpressing, respectively. At least six leaf discs were measured from each treatment using a luminolbased chemiluminescence assay. RLU, relative luminescence units. Data are presented as the mean  $\pm SD$  (n = 3). (d) The transcript levels of antioxidant enzyme genes encoding ascorbate peroxidase (APX), superoxide dismutase (FeSOD) and glutathione reductase (GR) were quantified by reverse transcription-quantitative PCR assay in TRV-GFP and TRV-NbRBP3 silenced plants treated with 10μM flg22. Results were presented as the mean  $\pm$  SD (n = 3). Asterisks represent significance levels determined by Student's t-test (\*\*\*p < 0.001) compared to the controls. (e) Fluorescence probe CM- $H_2$ DCFDA was used to detect reactive oxygen species in TRV-GFP and TRV-NbRBP3 silenced plants treated with 10 μM flg22. Scale bars = 40 μm. For the fluorescence intensity analysis, three pictures from each group were analysed using ImageJ. The results were the mean ± SD of three pictures. Asterisks represent significance levels determined by Student's t-test (\*\*\*p < 0.001) compared to the controls.

3643703, 2024, 1, Downloaded from https://bsppjournals

onlinelibrary.wiley.com/doi/10.1111/mpp.13416 by Readcube-Labtiva.

Wiley Online Library on [20/09/2025]. See the Terms

QA A

 $NbRBP3a\Delta N$ -CGFP did not significantly change lesion sizes compared to the GFP plants (Figure 3b), showing that the RRM motif is required for the immune function of NbRBP3a. Consistent results were obtained in the biomass quantification, where the NbRBP3a-CGFP and  $NbRBP3a\Delta C$ -CGFP overexpression leaves had less P. infestans biomass compared to the GFP overexpression leaves (Figure 3b), while  $NbRBP3a\Delta N$ -CGFP plants showed a similar amount. In conclusion, our results demonstrated that the RRM motif of NbRBP3a is important for the mechanisms of plant defence against P. infestans.

To further reveal the role of NbRBP3a in the plant PTI response, we examined whether it participated in ROS bursts to strengthen plant immunity. Using a luminol-based chemiluminescence assay, ROS production was examined in TRV-NbRBP3 silenced plants, as well as plants transiently overexpressing NbRBP3a-CGFP and its mutants. The results showed that silencing of NbRBP3 restricted ROS accumulation (Figure 3c), while transient overexpression of NbRBP3a-CGFP and  $NbRBP3a\Delta C$ -CGFP resulted in higher ROS levels compared with the GFP leaves (Figure 3c). Overexpression of  $NbRBP3a\Delta N$ -CGFP showed no significant increase in ROS levels compared with the control. These results suggested that the NbRBP3a protein may regulate plant immunity through the induction of ROS bursts.

RT-qPCR assays were used to examine the transcript levels of PTI and SA marker genes in TRV-NbRBP3 silenced plants and the control TRV-GFP silenced plants that had both been treated with flg22. The results showed that compared with the control TRV-GFP silenced plants, the expression levels of WRKY7, WRKY8, PR1 and PR2 were dramatically decreased in the TRV-NbRBP3 silenced plants (Figure S12), suggesting that NbRBP3a functions as a positive regulator of plant PTI responses. To evaluate the expression of ROS scavenging genes encoding ascorbate peroxidase (APX), superoxide dismutase (FeSOD) and glutathione reductase (GR) (Liu et al., 2021), the TRV-NbRBP3 silenced plants were treated with flg22 and collected at 3h after treatment for RT-qPCR assays. Compared with the control TRV-GFP silenced plants, the expression levels of APX, FeSOD and GR were dramatically increased in the TRV-NbRBP3 silenced plants (Figure 3d), indicating that silencing NbRBP3 restricted ROS accumulation by up-regulating antioxidant genes. The fluorescent probe oxidized dichlorofluorescein (CM-H<sub>2</sub>DCFDA) was used for monitoring ROS formation and localization in TRV-NbRBP3 silenced plants treated with flg22. Using confocal microscopy, the CM-H<sub>2</sub>DCFDA signal was observed in the cytoplasmic membranes, nucleus and chloroplasts in TRV-GFP silenced plants, while weak signal accumulated in TRV-NbRBP3 silenced plants compared to that in the TRV-GFP silenced plants (Figures 3e and S13), indicating that silencing NbRBP3 may suppress PTI-induced ROS bursts. These results suggested that silencing NbRBP3 negatively regulated the PTI signalling pathway.

# 2.4 | PSII activity was reduced in the TRV-NbRBP3 silenced plants

RBPs play an important role in chloroplast function (Ma et al., 2022). It has been shown that RBPs are able to regulate the stability and

translation of chloroplast mRNA, especially in response to light (Marondedze et al., 2016). SIRBP1, which accumulated in the nucleus and cytoplasm, is indispensable for photosynthesis and chloroplast function (Ma et al., 2022). NbRBP3a was localized to the nucleus and cytoplasm (Figure 2). Because PSII is vital for chloroplast, its destruction leads to a significant reduction in plant productivity, which hinders the plant ability to adapt to changing conditions (Wang et al., 2016). We also found that the TRV-NbRBP3 silenced plants showed mottled yellow leaves and retarded growth (Figures S10 and S11).

To investigate whether the NbRBP3a protein affects PSII function, we examined TRV-NbRBP3 silenced plants using a chlorophyll fluorescence video imaging system. The electron transport rate (ETR) (Ghosh et al., 2017), actual quantum yield of PSII (Y(II)), redox state of the QA electron acceptor of PSII (1-qP) and nonphotochemical quenching (NPQ) (Brabandt et al., 2014) were used to analyse the photosynthetic activity of different plants infected with pathogens, which elucidated the effect of pathogen infections on PSII activity (de Torres Zabala et al., 2015; Littlejohn et al., 2021). The results showed that TRV-NbRBP3 silenced plants displayed a lower maximum quantum yield of PSII (Fv/Fm) compared to the TRV-GFP silenced plants (Figures 4a and S11). Indeed, the Y(II) and ETR values were much lower in TRV-NbRBP3 silenced plants compared to the TRV-GFP silenced plants (Figure 4a). 1-qP and NPQ were found to be notably higher in the TRV-NbRBP3 silenced plants (Figure 4a), suggesting a more highly oxidized plastoquinone pool in the plants. These results indicated that silencing NbRBP3 affects PSII photosynthetic efficiency. We also found the transcript levels of PSII-related genes PsbA, PsbB, PsbC, PsbD and PsbE were dramatically decreased in TRV-NbRBP3 silenced plants during P. infestans infection (Figure 4b). This result suggested that silencing NbRBP3 negatively regulated the expression of PSII-associated genes. The expression of PSI-associated gene PsaA and chloroplast ATPB were up-regulated by at least twofold in the TRV-NbRBP3 silenced plants compared with the control TRV-GFP silenced plants (Figure 4b).

Singlet oxygen (1O2) accumulates in the chloroplast, mitochondria, peroxisome and nucleus (Mor et al., 2014; Wang & Klaus, 2018), leading to lipid peroxidation and reduced photosynthetic activity (Havaux, 2014; Kachroo et al., 2021; Kuniak & Kopczewski, 2020). In addition, <sup>1</sup>O<sub>2</sub> oxidated extension factor inhibited the D1 protein (PsbA) of PSII, affected PSII repair and destroyed PSII activity (Stael et al., 2015; Wang et al., 2016). RT-qPCR assays showed that the expression levels of EXECUTER 1 (EX1), EX2 and SIGMA FACTOR BINDING PROTEIN1 (SIB1) that mediate <sup>1</sup>O<sub>2</sub> signalling pathways were significantly up-regulated in the TRV-NbRBP3 silenced plants compared with the control during P. infestans infection (Figure 4c). The result indicated that silencing NbRBP3 facilitated <sup>1</sup>O<sub>2</sub> generation. By using singlet oxygen sensor green (SOSG) to detect <sup>1</sup>O<sub>2</sub> generation, the results showed that TRV-NbRBP3 silenced plants produced the maximum SOSG fluorescence in their nucleus and cytosol surrounding the chloroplasts. This is most probably caused by leakage from the organelle, with no SOSG signals in nucleus and cytosol of the control plants (Figures 4d and S14). These results

13643703, 2024, 1, Downloa

onlinelibrary.wiley.com/doi/10.1111/mpp.13416 by Readcube-Labtiva, Wiley Online Library on [20/09/2025]. See the Terms and Condit

of use; OA articles are governed by the applicable Creative Commons License

FIGURE 4 TRV-NbRBP3 silenced plants showed reduced photosystem II (PSII) activity and activated  ${}^{1}O_{2}$  signalling pathway. (a) Fv/Fm quantitation to indicate inhibition of photosynthesis in TRV-NbRBP3 silenced plants. Results were presented as the mean  $\pm$  SD of three leaves. Asterisks above the bars indicate significant differences based on Student's t-test (\*\*p<0.01). PSII light-response curves for electron transfer rate (ETR), photosynthetic quantum yield (Y(II)), the redox state of the QA electron acceptor of PSII (1-qP) and non-photochemical quenching (NPQ) in the TRV-GFP and TRV-NbRBP3 silenced plants. Measurements were performed at light intensities of 0, 27, 35, 53, 72, 111, 149, 189, 231, 289, 347, 438, 518, 628, 776, 940 and 1195  $\mu$ mol photons·m $^{-2}$ ·s $^{-1}$ . (b, c) The expression of PSII-related genes, EX1, EX2 and SIB1 were detected in TRV-NbRBP3 silenced plant leaves during Phytophthora infestans infection as quantified by reverse transcription-quantitative PCR assay. Results were presented as the mean  $\pm$  SD of three replicates. The asterisks indicate significant differences based on Student's t-test (\*\*\*p<0.001). (d) Quantification of  $^{1}O_{2}$  using the  $^{1}O_{2}$  sensor green (SOSG) assays. Scale bars = 40  $\mu$ m. For the fluorescence intensity analysis, three pictures from each group were analysed using ImageJ. The results were the mean  $\pm$  SD of three pictures. Statistical significance was assessed by Student's t-test. \*\*\*p<0.001.

.3643703, 2024, 1, Downloaded from https://bsppjournals

onlinelibrary.wiley.com/doi/10.1111/mpp.13416 by Readcube-Labtiva, Wiley Online Library on [20/09/2025]. See the Terms

of use; OA articles are governed by the applicable Creative Comm

indicated that silencing *NbRBP3* specifically attenuated photosynthesis, suppressed photosynthetic activity of PSII and increased  $^{1}O_{2}$  accumulation.

# 2.5 | Silencing *NbRBP3* attenuated Pi23014mediated suppression of *INF1*-triggered cell death

Pi23014 was shown to attenuate cell death triggered by the expression of INF1, BAX, R1/Avr1 and R3a/Avr3aKI (Figure 5), which suggested that Pi23014 may regulate the recognition of diverse factors that lead to cell death. To investigate whether the ability of Pi23014 to attenuate cell death is dependent on NbRBP3a, we transiently co-expressed the necrosis inducers and Pi23014 by agroinfiltration in the TRV-NbRBP3 and TRV-GFP silenced plants, respectively. As shown in Figure 5, Pi23014 expression still mitigated cell death triggered by BAX, R1/Avr1 and R3a/Avr3a<sup>KI</sup> in both the TRV-NbRBP3 silenced plants and the TRV-GFP silenced plants. However, there was no significant difference in cell death induced by INF1 compared with that of co-expression of the Pi23014 and INF1 in the TRV-NbRBP3 silenced plants. Co-expression of INF1 and Pi23014 inhibited cell death in the TRV-GFP silenced plants (Figure 5). In addition, silencing NbRBP3 did not influence cell death triggered by BAX, INF1 and R1/Avr1 and R3a/Avr3a<sup>KI</sup>, indicating that NbRBP3a was not involved in the cell death triggered by recognition of diverse factors.

These results suggested that *NbRBP3a* was involved in the Pi23014-mediated suppression of *INF1*-triggered cell death in *N. benthamiana*.

# 3 | DISCUSSION

RBPs play an important role in the regulation of fine gene expression at the transcriptional and post-transcriptional levels, which are key for regulating plant growth, development and stress response (Lee & Kang, 2016; Zuo et al., 2019). RBPs are rigorously regulated and reshaped in response to changes in environmental conditions and cellular states. Over the past few decades, identification and functional characterization of RBPs in different species using genetic and biochemical methods have improved our understanding of RBPs in different cellular processes (Lee & Kang, 2016).

Effectors regulate plant immunity and may target multiple plant factors, participating in various immune responses. In our mass spectrometry results, NbRBP3a and Pi23014 were found to have high coverage. We confirmed Pi23014 interaction with NbRBP3a using multiple assays, including LCI, Co-IP and Y2H (Figure 1). Both co-localization and bimolecular fluorescence complementation assays indicated that Pi23014 and NbRBP3a associate in the nucleus.

BAX is a proapoptotic member that can translocate into the mitochondrial membrane, triggering the apoptotic process. INF1 is a secreted elicitin that exists widely in *Phytophthora* and triggers

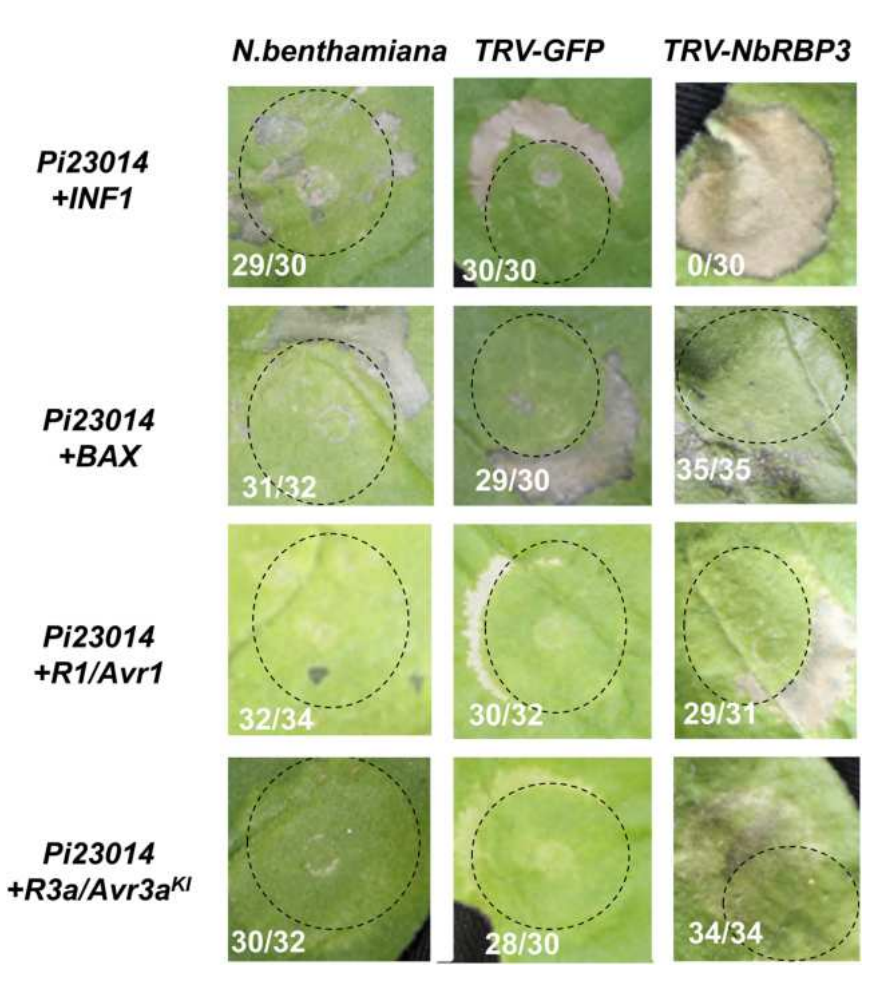


FIGURE 5 NbRBP3a was required for Pi23014-mediated suppression of cell death triggered by Phytophthora infestans elicitor INF1. Agrobacterium tumefaciens GV3101 cells carrying Pi23014-CGFP were mixed with cells carrying elicitor constructs and were co-infiltrated into TRV-GFP and TRV-NbRBP3 silenced plant leaves (at least 10 leaves). Phenotypic changes were scored at 4 days after agroinfiltration. The ratios next to the infiltrated zones indicate the number of infiltration sites with no cell death versus the total number of infiltration sites.

3643703, 2024, 1, Downloaded from https://bsppjournals

onlinelibrary.wiley.com/doi/10.1111/mpp.13416 by Readcube-I

Wiley Online Library on [20/09/2025]. See the Terms

QA A

cell death in N. benthamiana (Lu et al., 2020). Strikingly, silencing NbRBP3 prevented Pi23014 suppression of INF1-mediated cell death (Figure 5), revealing the ability of Pi23014 to attenuate cell death triggered by INF1 is dependent on NbRBP3a.

Plants require complex transcriptome control to regulate biological processes in response to a changing environment. RBPs are the centres of post-transcriptional regulation, contributing to the stabilization of RNA transcription maturation and serving as key regulatory steps that enable plants to adapt to these endless changes in the environment (Prall et al., 2019). More and more RBPs have been shown to be involved in regulating plant immunity. CPR5, a key immunomodulator in Arabidopsis thaliana, is a novel RBP that forms a complex with RNA processing regulators NTC and CPSF. Genome-wide profiling of RNA transcripts showed that CPR5 regulates roughly 500 alternatively spliced genes, which may determine the specificity and strength of plant immunity to a variety of microorganisms (Peng et al., 2022). RBP-DR1 contains three RRMs, all of which are involved in plant defence against P. syringae. Its overexpression leads to increased SA levels (Qi et al., 2010). The SAmediated defence response restricts the spread of biotrophic and hemibiotrophic pathogens (Yang et al., 2021), and ROS and SA signalling pathways reinforce each other to amplify immune signals (Nie et al., 2015). The RRM containing flowering regulator FPA regulates 3'-terminus mRNA polyadenylation, negatively regulates Arabidopsis resistance to the bacterial pathogen P. syringae, and inhibits PTI (Lyons et al., 2013).

RT-qPCR assays showed that the expression of NbRBP3a was induced during P. infestans infection in N. benthamiana, while transient overexpression of NbRBP3a rendered the plant more resistant to the pathogen. In addition, RT-qPCR analyses showed that the expression of marker genes for multiple defence pathways was significantly down-regulated in the TRV-NbRBP3 silenced plants compared with the TRV-GFP silenced plants under flg22 treatment, demonstrating that silencing NbRBP3 negatively affected plant immunity. We also found that NbRBP3a affects ROS to enhance plant immunity. Mutation of the RRM of N-terminus NbRBP3a abolished interaction with Pi23014. Moreover, our data demonstrated that NbRBP3a∆C protein is a positive regulator of plant immunity to P. infestans and NbRBP3a\Delta N protein no longer weakens leaf colonization by P. infestans, implying that the RNA recognition motif is probably required for this activity (Figure 3). Taken together, these data indicate that NbRBP3a plays an important role in plant defence through its RRM motif.

RBPs play an important role in photosynthesis by affecting the stability and translation of chloroplast mRNA (Marondedze et al., 2016). The silencing of the GR-RBP gene SIRBP1 in tomato leads to severely damage chloroplast ultrastructures and a decrease in photosynthetic activity (Ma et al., 2022), indicating that SIRBP1 is required for chloroplast function. Moreover, SIRBP1 binds photosynthesis-associated RNAs onto the translation initiation complex SleIF4A2 and facilitates the translation of RNAs to sustain chloroplast functions (Ma et al., 2022). Arabidopsis thaliana S1 RNAbound ribosomal protein 1 (SRRP1) also assists in RNA processing

and photosynthesis (Han et al., 2015). Therefore, we speculated that some RBPs could combine with chloroplast genes to regulate plant immunity.

The D1 protein of PSII is regulated by an RBP complex (Prall et al., 2019). Similarly, Chlamydomonas reinhardtii RBPNac21 binds to the 5' untranslated region of PsbD mRNA of PSII, effectively stabilizing it (Nickelsen et al., 1994). In tobacco chloroplasts, RNA-binding proteins (cpRBPs) exhibit a high affinity for poly(U)and poly(G) ribohomopolymers, and cp33 is necessary for stable accumulation of chloroplasts mRNAs. Similarly, tobacco cp31 participates in the editing process of PsbL mRNA (Mamoru & Masahiro, 1997). CSP41 proteins are likely to be metal-dependent ribonucleases that bind RNA and are critical to the proper regulation of chloroplast transcription, translation and RNA degradation (Bollenbach et al., 2009; Corredor-Moreno et al., 2022). RBPs can involve in regulating chloroplast biogenesis and photosynthesis (Han et al., 2015). PSII is one of the important components of the photosynthetic system (Kachroo et al., 2021). Environmental stressors on plants interfere with lightdriven photoelectron transport to produce highly active PSII disruptor, singlet oxygen, inhibiting photosynthesis and affecting plant growth (Dogra et al., 2018; Lu & Yao, 2018; Yang et al., 2021). More and more studies have shown that RBPs have an effect on the photosynthetic system.

Interestingly, we confirmed that the absence of NbRBP3a affected the activity of PSII. After silencing the NbRBP3a gene in N. benthamiana infected with TRV-NBRBP3, the plants had yellow leaves. PSII quantum yield (Y(II)), maximum quantum yield (Fv/Fm), electron transport rate (ETR) and non-photochemical quenching (NPQ) have been used to analyse photosynthetic activity in different plant species infected with downy mildew and powdery mildew (Brabandt et al., 2014). Chlorophyll fluorescence analysis showed that silencing NBRBP3 decreased the activity of PSII and resulted in a decrease in photosynthesis. Silencing NBRBP3 affected the expression of PSII-related genes. We also detected the expression levels of <sup>1</sup>O<sub>2</sub>-related genes EX1, EX2 and SIB1 by RT-gPCR. Compared with TRV-GFP silenced plants, inoculation of TRV-NBRBP3 silenced plants with P. infestans produced more <sup>1</sup>O<sub>2</sub> (Figure 4). Our result showed that TRV-NbRBP3 silenced plants produced more SOSG fluorescence in their nucleus and cytosol surrounding the chloroplasts than the control plants (Figure 4). These results showed that NbRBP3a is also involved in regulating PSII activity in response to the <sup>1</sup>O<sub>2</sub> signalling pathway. Therefore, we speculated that NbRBP3a may be involved in the regulation of PSII-related protein RNA to regulate photosynthesis and affect plant immunity.

Regulation of plant immunity is achieved by binding RBPs that directly or indirectly target RNA (Prall et al., 2019). The RBP BSR-K1, facilitates the overturn of the defence-related OsPAL gene by binding to its mRNA. Loss of BSR-K1 function causes reduced mRNA conversion, resulting in the accumulation of OsPAL transcripts in BSR-K1 mutants, which increases the resistance of BSR-K1 mutants to all tested M. oryzae isolates (Zhou et al., 2018). However, whether this nuclear protein NbRBP3a specifically controls its RNA targets to maintain chloroplast function during plant growth, development and

immunity, remains unclear. Natural RNA immunoprecipitation and high-throughput sequencing (NRIP-SEQ) technology will be useful methods to identify NbRBP3a-associated specific RNA targets. It will also be useful to further understand mechanisms of translation regulation and obtain new immune-related components. Our work has implications for improving agricultural plant productivity by repairing PSII.

In summary, our results revealed that NbRBP3a is a target of *P. infestans* virulence effector Pi23014 and positively regulates plant resistance to *P. infestans* by activating PTI. Silencing *NbRBP3* in plants reduced PSII activities, reduced host photosynthetic efficiency and suppressed plant immunity (Figure 6). We also found that *NbRBP3a* is required for Pi23014-mediated suppression of PTI responses (Figure 6), which offers a promising target to be further explored in plant breeding to improve crop resistance against pathogens. Pi23014 may inhibit the function of NbRBP3a, allowing for the promotion of infection. A comprehensive understanding of the mechanisms underlying effector–RBP interactions is required to improve plant disease resistance and photosynthesis.

# 4 | EXPERIMENTAL PROCEDURES

#### 4.1 | Plasmid constructs

P. infestans RXLR effector gene Pi23014 was cloned without the signal peptide from gDNA of isolate T30-4 to the coding sequence and NbRBP3a, NbRBP3a∆C and NbRBP3a∆N were amplified from N. benthamiana cDNA. To prepare overexpression constructs, Pi23014-CGFP, NbRBP3a-CGFP, NbRBP3a∆C-CGFP and NbRBP3a∆N-CGFP plasmids were generated in a similar way using XhoI and XbaI sites into pART27 vector. NbRBP3a-CmCherry, NbRBP3a∆C-CmCherry and NbRBP3a∆N-CmCherry plasmids were generated using EcoRI and Xbal sites into pART27-NmCherry vector, respectively. For LCI assays, Pi23014 and NbRBP3a, NbRBP3aΔC and NbRBP3aΔN were inserted into pCAMBIA-NLuc and pCAMBIA-CLuc using BamHI and SalI sites to form the nlucPi23014 and clucNbRBP3a, clucNbRBP3a\C and clucNbRBP3a\Delta N plasmids, respectively. For Y2H assays, Pi23014 was cloned into the pGBKT7 vector (Fan et al., 2018) using EcoRI and BamHI sites to form the plasmid. BDPi23014. NbRBP3a,

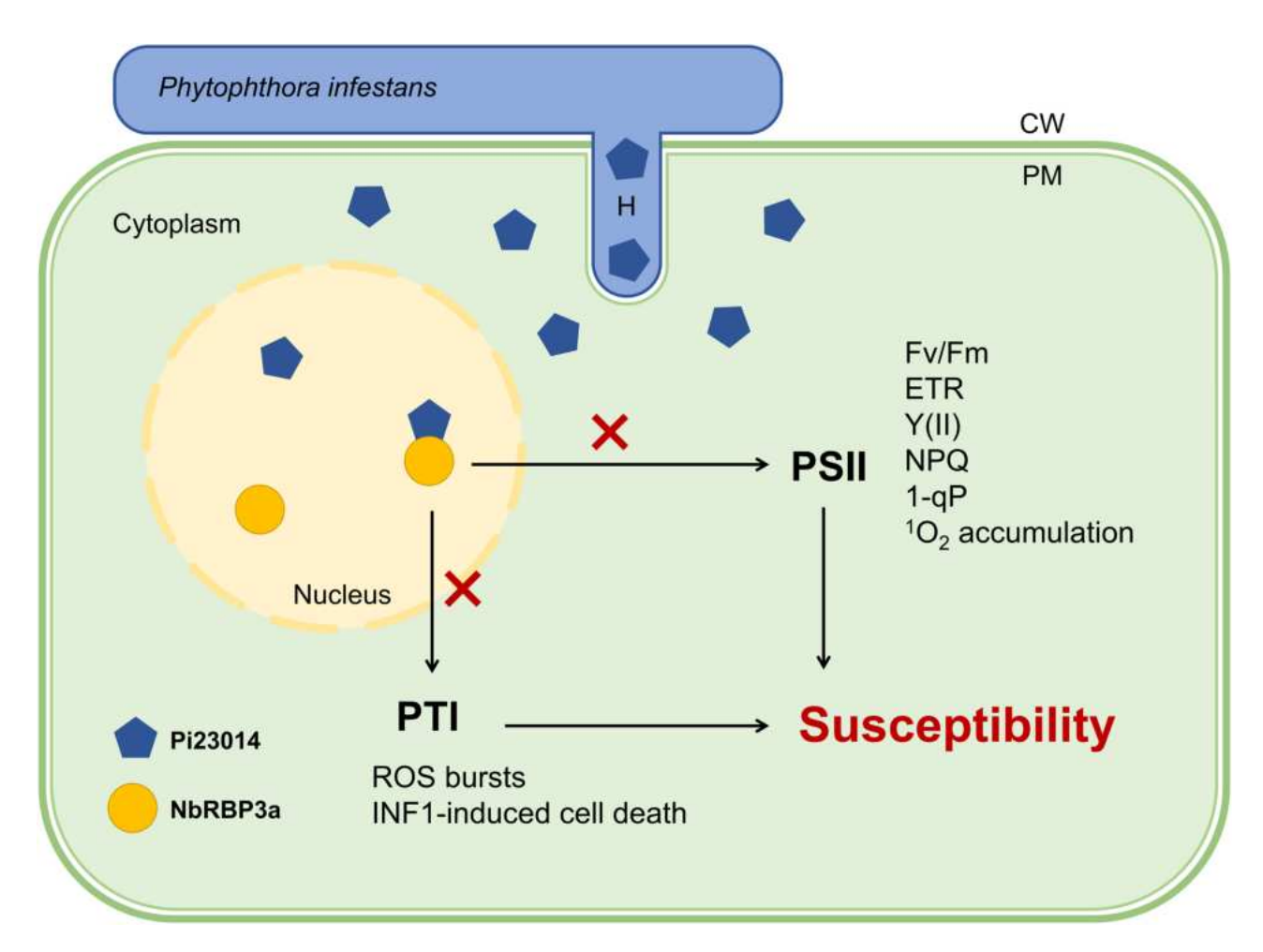


FIGURE 6 Model of the Pi23014-mediated suppression of host photosystem II (PSII) activity to promote plant susceptibility. The *Phytophthora infestans* effector Pi23014 targets NbRBP3a to inhibit PAMP-triggered immunity (PTI) responses and PSII activity, leading to promote plant susceptibility. Protecting chloroplasts PSII activity from the effects of pathogen effectors is therefore a potential strategy for developing crop disease resistance. CW, cell wall; H, haustorium; PM, plasma membrane; PSII, photosystem II; ROS, reactive oxygen species.

3643703, 2024, 1, Downloaded from https://bsppjo

onlinelibrary.wiley.com/doi/10.1111/mpp.13416 by Readcube-Labtiva,

Wiley Online Library on [20/09/2025]. See the Terms

on Wiley Online Library for rules

of use; OA articles are governed by the applicable Creative Commons License

 $NbRBP3a\Delta C$  and  $NbRBP3a\Delta N$  were cloned into the pGADT7 using EcoRI and XhoI sites to form the ADNbRBP3a, ADNbRBP3a $\Delta C$  and ADNbRBP3a $\Delta N$  plasmids, respectively. For BiFC assays, Pi23014 was cloned into pDEST-VYNE(R) vector (Fan et al., 2018) using Spel and XhoI sites to form the nYFP-Pi23014 plasmid. NbRBP3a,  $NbRBP3a\Delta C$  and  $NbRBP3a\Delta N$  were cloned into pDEST-VYCE(R) vector using Spel and XhoI sites to form the cYFP-NbRBP3a, cYFP-NbRBP3a $\Delta C$  and cYFP-NbRBP3a $\Delta N$  plasmids, respectively. For VIGS of NbRBP3 in N. benthamiana, a 300-bp fragment of NbRBP3 was chosen and amplified from N. benthamiana cDNA. The PCR product was inserted into pTRV2 with Xbal and BamHI sites. All the primers we used are listed in Table S2.

# 4.2 | Plant materials and growth conditions

N. benthamiana were planted and grown in small pots with nutrient soil (Pindstrup plus peat substrate), under 3000 lux illumination for 16 h in a growth chamber with a relative humidity of 50% at 23°C.

# 4.3 | Pathogen growth and infection assays

*P. infestans* culture conditions, zoospore production and the detached leaf inoculation assays were performed as described (Li et al., 2020). For the pathogenicity assays, the zoospore suspensions were adjusted to a concentration of 200 zoospores/µL. *N. benthamiana* leaves inoculated with *P. infestans* zoospores were scored and the lesion diameters were measured at 5 dpi. To observe the lesion size more clearly, trypan blue was used to stain the dead plant cells in lesions of inoculated leaves as described (Lu et al., 2020).

# 4.4 | RT-qPCR

Appropriate primers (Table S2) were used in  $10\,\mu$ L reactions, with the SYBR Green mix (CWBio) on an iQ7 Real-Time Cycler (Life Technologies). Three biological replicates were included in the assays. *NbActin* was measured as a housekeeping gene and expression fold changes were calculated via the  $2^{-\Delta\Delta Ct}$  method.

# 4.5 | Transient expression analysis and confocal microscopy observation

A. tumefaciens GV3101 transformed with vector constructs was incubated in liquid Luria Bertani medium with appropriate antibiotics at 28°C for 36 h. The bacteria were then harvested and resuspended in infiltration buffer (10 mM 2-[N-morpholino]ethane sulphonic acid MES, 10 mM MgCl $_2$ , 100 mM acetosyringone, pH 5.6) to the appropriate concentration for INF1 (OD $_{600}$ =0.1), BAX, R1/Avr1 and R3a/Avr3a $_{\rm K}$ 1 (OD $_{600}$ =0.15), confocal microscope observation, Co-IP,

infection assays ( $OD_{600}$ =0.2) and VIGS assays ( $OD_{600}$ =0.1). For co-expression assays, A. tumefaciens cultures carrying different vectors were mixed in a 1:1 ratio before infiltration. The N. benthamiana leaves were observed after infiltration by an Olympus FV3000 confocal microscope. GFP fluorescence was detected after excitation at 488 nm wavelength laser and emissions were collected between 500 nm to 540 nm. The fluorescence of mCherry was excited with a 561 nm wavelength laser to detect specific emissions between 600 nm and 680 nm.

### 4.6 | LCI assays

nlucPi23014 and clucNbRBP3a constructs were transformed into A. tumefaciens and the prepared agrobacterial cultures were mixed and infiltrated into N. benthamiana leaves. After 2 days, luciferase substrate (1 mM, beetle luciferin, potassium salt; Promega) was spread evenly over the agroinfiltration areas of leaves. After 5–10 min of dark treatment, in vivo imaging was performed using PlantView100.

# 4.7 Yeast two-hybrid assays

The plasmid vectors were co-transformed into yeast strain AH109. The yeast cells were cultivated at 30°C for 4h and collected by centrifugation at 1000g for 5 min. Transformations were tested on SD/–Leu/–Trp medium and interactions were confirmed by  $\beta$ -Gal activity on the QDO medium (Fan et al., 2018). Normal growth and blue colonies indicated the interaction of the co-transferred proteins.

### 4.8 | BiFC assays

The interaction proteins to be detected were examined by coagroinfiltration of fusion gene constructs into N. benthamiana leaves  $(OD_{600}=0.2)$ . After 2 days, the interaction was observed under a confocal microscope with an excitation light of 488 nm wavelength laser and emissions were collected between 500 nm to 540 nm. The fluorescence intensity was measured by ImageJ. After the image is added, a single channel is extracted (image-colour-split channels), and an appropriate threshold algorithm was selected (image-adjust-auto threshold). For the fluorescence intensity analysis, three images from each group were analysed using ImageJ. The results were the mean  $\pm SD$  of three pictures. Statistical significance was assessed by Student's t-test.

### 4.9 | Co-immunoprecipitation

After grinding the infiltrated N. benthamiana leaves, protein lysis buffer (10% glycerol, 25 mM Tris-HCl [pH7.5], 1 mM EDTA, 150 mM NaCl, 0.1% Tween 20, 0.1% NP40, 2% PVPP, 0.1 mM dithiothreitol,  $1 \times inhibitor cocktail$ ) was added. The total protein

Anti-mCherry antibody (Huxiang bio, HX1820, 1:5000 dilution) or anti-GFP antibody (Sigma, F3165, 1:10,000 dilution) was used to immunoblot analysis.

To perform the LC-MS/MS assay, three independent biological replicates were used to generate immunopurification samples. The enriched protein samples underwent freeze-drying, desalting and filter-aided sample preparation (FASP) for Orbitrap Fusion Lumos (Thermo Fisher) detection. The original downloaded data were directly submitted to the Proteinpilot software connected with the mass spectrometer for database retrieval. After the control GFP was removed, the remaining proteins were the candidate target proteins.

#### 4.10 Oxidative burst test

A luminol-based assay was used to detect ROS production. A 5 mm diameter hole puncher was used to punch the N. benthamiana leaves of transient gene expression to obtain 12 leaf discs. The leaf discs were floated in sterile ultrapure water in culture dishes overnight. The next day, the discs were transferred into 96-well plates, adding  $100 \mu L$  ECL kit luminol solution and  $100 \mu L$  of  $20 \mu g/mL$  horseradish peroxidase (Aladdin). Then, 5 μL of 41 μM flg22 was immediately added to each plate. ROS were measured using an Infinite M200 PRO (TECAN), selecting the kinetic cycle and 40 cycles for the measurement.

For CM-H2DCFDA staining assay, TRV-GFP and TRV-NbRBP3 silenced plants treated with 10 µM flg22 for 0.5h were stained with 10 μM CM-H<sub>2</sub>DCFDA for 0.5-1h to detect ROS, then washed twice before imaging (Yang et al., 2022). CM-H2DCFDA was excited at 488 nm with emission collected at 500-540 nm.

### Analysis of chlorophyll fluorescence

Chlorophyll fluorescence parameters (ETR, Y(II), 1-qP, NPQ) were measured using a DUALPAM chlorophyll fluorometer (Heinz-Walz Instruments) as previously described (Jin et al., 2018). To evaluate the maximum quantum yield (Fv/Fm) of PSII, all plants were adapted under darkness for 30 min and then imaged using the Imaging-PAM chlorophyll fluorescence system at room temperature (Effeltrich).

#### Determination of relative levels of <sup>1</sup>O<sub>2</sub> 4.12

The relative levels of <sup>1</sup>O<sub>2</sub> were monitored as described previously (Wang, Leister, et al., 2020). Leaves were immersed in a solution of 50-260μM Singlet Oxygen Sensor Green (SOSG) (Thermo Fisher Scientific) in 50 mM phosphate buffer (pH7.5), were vacuum infiltrated for 5 min and incubated for 2h in the dark, followed by imaging using a GFP filter in a FV3000 fluorescence microscope. The <sup>1</sup>O<sub>2</sub>-activated SOSG was visualized by excitation at 488nm and emission at 530 nm at room temperature.

#### **ACKNOWLEDGEMENTS**

This work was supported by the Agricultural Breeding program (2019NYYZ01) from the Ningxia Department of Science and Technology, China Agriculture Research System (CARS-09) and the Program of Introducing Talents of Innovative Discipline to Universities from the State of Administration for Foreign Experts Affairs, China (B18042).

#### CONFLICT OF INTEREST STATEMENT

The data that support the findings of this study are available from the corresponding author upon reasonable request.

#### DATA AVAILABILITY STATEMENT

The data that support the results are included in this article and its supplementary materials.

#### ORCID

Weixing Shan https://orcid.org/0000-0001-7286-4041

#### REFERENCES

- Bollenbach, T.J., Sharwood, R.E., Gutierrez, R., Lerbs-Mache, S. & Stern, D.B. (2009) The RNA-binding proteins CSP41a and CSP41b may regulate transcription and translation of chloroplast-encoded RNAs in Arabidopsis. Plant Molecular Biology, 69, 541-552.
- Brabandt, H., Bauriegel, E., GRber, U. & Herppich, W.B. (2014) PSII and NPQ to evaluate Bremia lactucae-infection in susceptible and resistant lettuce cultivars. Scientia Horticulturae, 180, 123-129.
- Corredor-Moreno, P., Badgami, R., Jones, S. & Saunders, D.G.O. (2022) Temporally coordinated expression of nuclear genes encoding chloroplast proteins in wheat promotes Puccinia striiformis f. sp. tritici infection. Communications Biology, 5, 853.
- de Torres Zabala, M., Littlejohn, G., Jayaraman, S., Studholme, D., Bailey, T., Lawson, T. et al. (2015) Chloroplasts play a central role in plant defence and are targeted by pathogen effectors. Nature Plants, 1,
- Dogra, V., Rochaix, J.D. & Kim, C. (2018) Singlet oxygen-triggered chloroplast-to-nucleus retrograde signalling pathways: an emerging perspective. Plant, Cell & Environment, 41, 1727-1738.
- Fan, G., Yang, Y., Li, T., Lu, W., Du, Y., Qiang, X. et al. (2018) A Phytophthora capsici RXLR effector targets and inhibits a plant PPlase to suppress endoplasmic reticulum-mediated immunity. Molecular Plant, 11, 1067-1083.
- Fu, Z., Guo, M., Jeong, B., Tian, F., Elthon, T.E., Cerny, R.L. et al. (2007) A type III effector ADP-ribosylates RNA-binding proteins and quells plant immunity. Nature, 447, 284-288.
- Ghosh, S., Kanwar, P. & Jha, G. (2017) Alterations in rice chloroplast integrity, photosynthesis and metabolome associated with pathogenesis of Rhizoctonia solani. Scientific Reports, 7, 41610.
- Han, J.H., Lee, K., Lee, K.H., Jung, S. & Kang, H. (2015) A nuclear-encoded chloroplast-targeted S1 RNA-binding domain protein affects chloroplast rRNA processing and is crucial for the normal growth of Arabidopsis thaliana. The Plant Journal, 83, 277-289.
- Havaux, M. (2014) Carotenoid oxidation products as stress signals in plants. The Plant Journal, 79, 597-606.
- Huang, J., Lu, X., Wu, H., Xie, Y., Peng, Q., Gu, L. et al. (2020) Phytophthora effectors modulate genome-wide alternative splicing of host mRNAs to reprogram plant immunity. Molecular Plant, 13, 1470-1484.
- Jin, H., Fu, M., Duan, Z., Duan, S., Li, M., Dong, X. et al. (2018) LOW PHOTOSYNTHETIC EFFICIENCY 1 is required for light-regulated

- photosystem II biogenesis in Arabidopsis. Proceedings of the National Academy of Sciences of the United States of America, 115, E6075-E6084.
- Jones, J.D. & Dangl, J.L. (2006) The plant immune system. Nature, 444, 323-329.
- Jong-Kuk, N., Jae-Kwang, K., Dool-Yi, K. & Assmann, S.M. (2015) Expression of potato RNA-binding proteins StUBA2a/b and StUBA2c induces hypersensitive-like cell death and early leaf senescence in Arabidopsis. Journal of Experimental Botany, 66, 4023-4033.
- Kachroo, P., Burch-Smith, T.M. & Grant, M. (2021) An emerging role for chloroplasts in disease and defense. Annual Review of Phytopathology, 59, 423-445.
- Kim, D.S., Kim, N.H. & Hwang, B.K. (2015) Glycine-rich RNA-binding protein1 interacts with receptor-like cytoplasmic protein kinase1 and suppresses cell death and defense responses in pepper (Capsicum annuum). New Phytologist, 205, 786-800.
- Kuniak, E. & Kopczewski, T. (2020) The chloroplast reactive oxygen species-redox system in plant immunity and disease. Frontiers in Plant Science, 11, 572686.
- Lee, K. & Kang, H. (2016) Emerging roles of RNA-binding proteins in plant growth, development, and stress responses. Molecules and Cells, 39, 179-185.
- Li, T., Xu, L., Chen, X., Feng, J., Wu, W., Du, Y. et al. (2022) StMPK7 phosphorylates and stabilizes a potato RNA-binding protein StUBA2a/b to enhance plant defence responses. Horticulture Research, 9, uhac177.
- Li, W., Zhao, D., Dong, J., Kong, X., Zhang, Q., Li, T. et al. (2020) AtRTP5 negatively regulates plant resistance to Phytophthora pathogens by modulating the biosynthesis of endogenous jasmonic acid and salicylic acid. Molecular Plant Pathology, 21, 95-108.
- Littlejohn, G.R., Breen, S., Smirnoff, N. & Grant, M. (2021) Chloroplast immunity illuminated. New Phytologist, 229, 3088-3107.
- Liu, R.Q., Chen, T.T., Yin, X., Xiang, G.Q., Peng, J., Fu, Q.Q. et al. (2021) A Plasmopara viticola RXLR effector targets a chloroplast protein PsbP to inhibit ROS production in grapevine. The Plant Journal, 106, 1557-1570.
- Lu, W., Deng, F., Jia, J., Chen, X., Li, J., Wen, Q. et al. (2020) The Arabidopsis thaliana gene AtERF019 negatively regulates plant resistance to Phytophthora parasitica by suppressing PAMP-triggered immunity. Molecular Plant Pathology, 21, 1179-1193.
- Lu, Y. & Yao, J. (2018) Chloroplasts at the crossroad of photosynthesis, pathogen infection and plant defense. International Journal of Molecular Sciences, 19, 3900.
- Lyons, R., Iwase, A., Gansewig, T., Sherstnev, A., Duc, C., Barton, G.J. et al. (2013) The RNA-binding protein FPA regulates flg22-triggered defense responses and transcription factor activity by alternative polyadenylation. Scientific Reports, 3, 2866.
- Ma, L., Yang, Y., Wang, Y., Cheng, K., Zhou, X., Li, J. et al. (2022) SIRBP1 promotes translational efficiency via SleIF4A2 to maintain chloroplast function in tomato. The Plant Cell, 34, 2747-2764.
- Mahalingam, R. & Walling, J.G. (2020) Genomic survey of RNA recognition motif (RRM) containing RNA binding proteins from barley (Hordeum vulgare ssp. vulgare). Genomics, 112, 1829-1839.
- Mamoru, S. & Masahiro, S. (1997) Chloroplast RNA-binding proteins. Nippon Nōgeikagaku Kaishi, 71, 1177-1179.
- Manavski, N., Schmid, L.M. & Meurer, J. (2018) RNA-stabilization factors in chloroplasts of vascular plants. Essays in Biochemistry, 62, EBC20170061.
- Marondedze, C., Thomas, L., Serrano, N.L., Lilley, K.S. & Gehring, C. (2016) The RNA-binding protein repertoire of Arabidopsis thaliana. Scientific Reports, 6, 29766.
- Mor, A., Koh, E., Weiner, L., Rosenwasser, S., Sibony-Benyamini, H. & Fluhr, R. (2014) Singlet oxygen signatures are detected independent of light or chloroplasts in response to multiple stresses. Plant Physiology, 165, 249-261.

- Ngou, B.P.M., Ahn, H.K., Ding, P. & Jones, J.D. (2021) Mutual potentiation of plant immunity by cell-surface and intracellular receptors. Nature, 592, 110-115.
- Nicaise, V., Joe, A., Jeong, B.R., Korneli, C., Boutrot, F., Westedt, I. et al. (2013) Pseudomonas HopU1 modulates plant immune receptor levels by blocking the interaction of their mRNAs with GRP7. The EMBO Journal, 32, 701-712.
- Nickelsen, J., Van Dillewiin, J., Rahire, M. & Rochaix, J.D. (1994) Determinants for stability of the chloroplast psbD RNA are located within its short leader region in Chlamydomonas reinhardtii. The EMBO Journal, 13, 3182-3191.
- Nie, S., Yue, H., Zhou, J. & Xing, D. (2015) Mitochondrial-derived reactive oxygen species play a vital role in the salicylic acid signaling pathway in Arabidopsis thaliana. PLoS One, 10, e0119853.
- Oca, S., Zheng, Q., Ej, S., Mekken, M., Mendel, M., Putker, V. et al. (2022) Glycine-rich RNA-binding protein 7 potentiates effector-triggered immunity through an RNA recognition motif. Plant Physiology, 189, 972-987.
- Peng, S., Guo, D., Guo, Y., Zhao, H., Mei, J., Han, Y. et al. (2022) Constitutive expresser of pathogenesis-related genes 5 is an RNAbinding protein controlling plant immunity via an RNA processing complex. The Plant Cell, 34, 1724-1744.
- Prall, W., Sharma, B. & Gregory, B.D. (2019) Transcription is just the beginning of gene expression regulation: the functional significance of RNA-binding proteins to post-transcriptional processes in plants. Plant Cell Physiology, 60, 1939-1952.
- Qi, Y.P., Tsuda, K., Joe, A., Sato, M., Nguyen, L.V., Glazebrook, J. et al. (2010) A putative RNA-binding protein positively regulates salicylic acid-mediated immunity in Arabidopsis. Molecular Plant-Microbe Interactions, 23, 1573-1583.
- Stael, S., Kmiecik, P., Willems, P., Van, D. & Van, B. (2015) Plant innate immunity-sunny side up? Trends in Plant Science, 20, 3-11.
- Tang, Y., Huang, C., Li, Y., Wang, Y. & Zhang, C. (2021) Genome-wide identification, phylogenetic analysis, and expression profiling of glycine-rich RNA-binding protein (GRPs) genes in seeded and seedless grapes (Vitis vinifera). Physiology and Molecular Biology of Plants, 27, 2231-2243.
- Tsuda, K. & Lu, Y. (2020) Intimate association of PRR- and NLR-mediated signaling in plant immunity. Molecular Plant-Microbe Interactions, 34,
- Wang, L., Kim, C., Xu, X., Piskurewicz, U., Dogra, V., Singh, S. et al. (2016) Singlet oxygen- and EXECUTER1-mediated signaling is initiated in grana margins and depends on the protease FtsH2. Proceedings of the National Academy of Sciences of the United States of America, 113, E3792-E3800.
- Wang, L. & Klaus, A. (2018) Dose-dependent effects of <sup>1</sup>O<sub>2</sub> in chloroplasts are determined by its timing and localization of production. Journal of Experimental Botany, 70, 29-40.
- Wang, L., Leister, D., Guan, L., Zheng, Y., Schneider, K., Lehmann, M. et al. (2020) The Arabidopsis SAFEGUARD1 suppresses singlet oxygeninduced stress responses by protecting grana margins. Proceedings of the National Academy of Sciences of the United States of America, 117, 6918-6927.
- Wang, S., McLellan, H., Bukharova, T., He, Q., Murphy, F., Shi, J. et al. (2019) Phytophthora infestans RXLR effectors act in concert at diverse subcellular locations to enhance host colonization. Journal of Experimental Botany, 70, 343-356.
- Wang, W., Feng, B., Zhou, J.M. & Tang, D. (2020) Plant immune signaling: advancing on two frontiers. Journal of Integrative Plant Biology, 62, 2-24.
- Wang, X., Boevink, P., Mclellan, H., Armstrong, M., Bukharova, T., Qin, Z. et al. (2015) A host KH RNA-binding protein is a susceptibility factor targeted by an RXLR effector to promote late blight disease. Molecular Plant, 8, 1385-1395.
- Xu, T., Lee, H.J., Sy, N.D. & Kang, H. (2015) Wheat (Triticum aestivum) zinc finger-containing glycine-rich RNA-binding protein TaRZ1 affects

- plant growth and defense response in Arabidopsis thaliana. Plant Growth Regulation, 76, 243–250.
- Yang, F., Xiao, K.Q., Pan, H.Y., Liu, J.L. et al. (2021) Chloroplast: the emerging battlefield in plant-microbe interactions. Frontiers in Plant Science, 12, 637853.
- Yang, Y., Zhao, Y., Zhang, Y., Niu, L., Li, W., Lu, W. et al. (2022) A mitochondrial RNA processing protein mediates plant immunity to a broad spectrum of pathogens by modulating the mitochondrial oxidative burst. *The Plant Cell*, 34, 2343–2363.
- Zhai, K., Deng, Y., Liang, D., Tang, J., Liu, J., Yan, B. et al. (2019) RRM transcription factors interact with NLRs and regulate broad-spectrum blast resistance in Rice. *Molecular Cell*, 74, 996–1009.
- Zhang, F., Fang, H., Wang, M., He, F., Tao, H., Wang, R. et al. (2022) APIP5 functions as a transcription factor and an RNA-binding protein to modulate cell death and immunity in rice. *Nucleic Acids Research*, 50, 5064–5079.
- Zhou, X., Liao, H., Chern, M., Yin, J., Chen, Y., Wang, J. et al. (2018) Loss of function of a rice TPR-domain RNA-binding protein confers broad-spectrum disease resistance. *Proceedings of the National Academy of Sciences of the United States of America*, 115, 3174–3179.

Zuo, Y., Feng, F., Qi, W. & Song, R. (2019) Dek42 encodes an RNA-binding protein that affects alternative pre-mRNA splicing and maize kernel

#### SUPPORTING INFORMATION

Additional supporting information can be found online in the Supporting Information section at the end of this article.

development. Journal of Integrative Plant Biology, 61, 728-748.

How to cite this article: Li, W., Liu, Z., Huang, Y., Zheng, J., Yang, Y., Cao, Y. et al. (2024) *Phytophthora infestans* RXLR effector Pi23014 targets host RNA-binding protein NbRBP3a to suppress plant immunity. *Molecular Plant Pathology*, 25, e13416. Available from: <a href="https://doi.">https://doi.</a>

org/10.1111/mpp.13416